Journal of the Korean Nuclear Society
Volume 22, Number 4, December 1990

A Comparison of Low-Dimensional Reactor Kinetics Analysis Methods with Modified Borresen's Coarse-Mesh Method

Chang Hyo kim Gyu Bok Lee
Seoul National University
Korea Atomic Energy Research Institute

(Received May 10, 1990)

저차원 원자로 동특성 해법과 다차원 수정형 Borresen 소격해법의 비교

김창효 · 이규복
서울대학교

(1990. 5. 10 접수)

Abstract

This study concerns with comparing low-dimensional reactor kinetics methods with a three-dimensional kinetics method to be used for safety analysis of light water reactors in order to suggest means of preparing input parameters required for low-dimensional methods. For this purpose a one-dimensional finite difference two-group diffusion theory code ODTRAN and a third-order Hermite polynomial-based point kinetics code POTRAN are developed and used to obtain low-dimensional solutions to the LRA-BWR kinetics benchmark problem. The results are compared with a three-dimensional modified Borresen's coarse-mesh solution of the kinetics problem by CMSNACK code. Through this comparison some simple but practical means of preparing input parameters of low-dimensional kinetics analysis methods are suggested.

요 약

이 논문은 원자력발전소의 안전사고해석에 흔히 이용되는 중성자 다군확산 동특성방정식의 저차원(0차원 및 1차원) 수치해를 3차원 수치해와 비교함으로써 저차원 수치해법에 요구되는 동특성해석 입력자료를 체계적으로 유도하기 위한 것이다. 이 목적으로 이 논문에서는 수정형 Borresen 소격모형에 의한 3차원 동특성 해석코드인 CMSNACK 전산코드로 LRA-BWR 경수로 동특성 시범문제의 3차원해를 구하고 이 해를 기준으로 삼아 중성자 다군확산 동특성방정식의 1차원 유한차분해와 3차 Hermit 다항식 전개해법에 의한점운동방정식의 0차원 수치해를 비교하고자 했다

중성자 다군확산방정식의 1차원 유한차분해와 점운동방정식의 0차원 수치해를 구하기 위해 ODTRAN 전산코드와 POTRAN 전산코드를 개발하였고 이들 코드의 입력자료는 ODTRAN 코드의 경우 중성자속 체적가중법을 POTRAN의경우 단열근사법을 수정하여 마련하였다. 이같이 마련한 입력자료를 써서 LRA-BWR 동특성문제에 대한 1차원 및 0차원 해를 구했으며 그 결과를

CMSNACK 코드에 의한 3차원 해와의 비교를 통해서 저차원 수치해의 계산효율성과 안전해석코드에 요구되는 계산결과의 보수성등을 조사했다. 이같은 비교결과를 토대로 저차원 수치해법의 입력자료 마련에 이 논문에서 제시한 방법이 유용하게 이용될 수 있음을 보였다.

1. Introduction

In the safety analysis of a certain light water reactor transients, modelling of the transient neutronic behavior by a three-dimensional(3-D) neutron kinetics equation is highly desirable for a satisfactory prediction of the transient results(1-3). Since heavy computational burden is generally involved in solving neutron kinetics equation in three dimension, low-dimensional methods such as point kinetics scheme and one-dimensional(1-D) group diffusion theory method are frequently adopted for modelling the neutronic behavior during the transient(4, 5).

From the computational standpoint, these low-dimensional methods are extremely efficient and therefore very useful for transient analysis, yet care must be exercised in preparing input parameters required for the methods in order to ensure computational accuracy of the transient analysis within acceptable degree(6). The purpose of this study is to examine predictability of low-dimensional kinetics methods in a light water reactor transient analysis in comparison with a reference 3-D kinetics method and thereby to suggest means to prepare input parameters required for low-dimensional methods to obtain acceptable computational accuracy.

For this purpose the LRA-BWR kinetics benchmark problem, which simulates a superprompt critical transient induced by a sudden withdrawal of control rod, is chosen(7). In order to obtain low-dimensional solutions to the LRA-BWR problem, ODTRAN code based on a finite difference solution of 1-D two group diffusion equation and POTRAN code based on a third-order Hermite polynomial solution of point kinetics equation are developed(8). The low-dimensional solutions of the LRA-BWR problem by the 1-D ODTRAN and the POTRAN code are compared with a 3-D reference solution by CMSNACK code which is based on a modified Borresen's coarse-mesh method(9). It is shown that low-dimensional methods can predict overall behavior of the LRA-BWR during the transient period in a fairly similar way as the 3-D method does and that computational accuracy depends on how to prepare the input parameters required for the methods.

2. Description of Neutron Kinetics Methods

In this section the modified Borresen's 3-D method and the low-dimensional methods are briefly described in order to show interrelationship between the 3-D solution and low-dimensional kinetics solutions.

2.1 The Modified Borresen's Coarse Mesh Scheme

This is one of the simplest coarse-mesh methods and is designed to obtain two-group flux $\phi g(r, t)$ (g=f, t or 1,2) on the 1.5 group principle. The equations to be solved in this scheme are finite difference nodal balance relations for the fast group diffusion density,

$$\phi_m^{(n)} = \sqrt{D_{fm}}\ \phi_{fm}^{(n)},$$

$$-\Sigma \psi_j^{(n)} + R\Sigma \psi_j^{(n)} + Q_m^{(n)} \psi_m^{(n)} = \frac{h_x^2}{(1-c_f q_m^{(n)})\sqrt{D_{fm}}} S_m^{(n)}, \quad (1)$$

where

$$S_m^{(n)} = \frac{1}{v_f \Delta t_n} \phi_{fm}^{(n-1)} + \Sigma_d \frac{\lambda_d}{1+\lambda_a \Delta t_n} C_{dn}^{(n-1)} + \frac{1}{k} (1 - \Sigma_d \frac{\beta_d}{1+\lambda_d \Delta t_n}) \times \upsilon \Sigma_{ftm} \bar{\phi}_{tm}^{(n)}, \quad (2a)$$

$$Q_m^{(n)} = \frac{P_m + (b_f + C_f r_m) q_m^{(n)}}{1 - C_f q_m^{(n)}}, \quad (2b)$$

$$q_m^{(n)} = \frac{h_x^2}{D_{fm}} \left\{ \frac{1}{v_f \Delta t_n} + \Sigma_{rm}^{(n)} - \frac{1}{k} (1 - \Sigma_d \frac{\beta_d}{1+\lambda_d \Delta t_n}) \upsilon \Sigma_{ffm} \right\}, \quad (2c)$$

$$p_m = \sum_{4j} \sqrt{\frac{D_{fi}}{D_{fm}}} + R \sum_{2j} \sqrt{\frac{D_{fi}}{D_{fm}}}, \quad (2d)$$

$$r_m = \sum_{4j} \sqrt{\frac{D_{fm}}{D_{fj}}} + R \sum_{2j} \sqrt{\frac{D_{fm}}{D_{fj}}} \quad (2e)$$

The $\psi_m^{(n)}$ is the fast group diffusion density at the center of the 3-D rectangular node m and at the time step n. The $\bar{\psi}_m^{(n)}$ and $C_{dm}^{(n)}$ are the nodal volume-averaged fast group diffusion density and the dth group delayed neutron precursor density for node m for the time step n. The other notations are the same as thoes in the original reference(9).

The source term of Eq.(1) contains nodal volume-averaged thermal group flux at the node m and time step tn, $\bar{\phi}_{tm}^{(n)}$. In the modified Borresen's method, this is approximated by an interpolation formular:

$$\bar{\phi}_{tm}(t) = b_{tm}(t) \phi_{tm}(t) + (\sum_{4j} \phi_{tmj}(t) + R \Sigma \phi^j_{tm}(t)), \quad (3)$$

in combination with an analytical expression for thermal group flux at the internodal surface, $\phi^j_{tm}(t)$,

$$\phi^j_{tm}(t) = \frac{\frac{D_{tm}K_m(t)}{T_m(t)} \phi_{tm}(t) + \frac{D_{tj}K_j(t)}{T_j(t)} \phi_{tj}(t)}{\frac{D_{tm}K_m(t)}{T_m(t)} + \frac{D_{tj}K_j(t)}{T_j(t)}} \quad (4)$$

where

$$K_m(t) = (\Sigma_{atm}(t) + \frac{W_m(t)}{\upsilon_{th}})/D_{tm}, \quad (5a)$$

$$T_m(t) = \tanh(K_m(t)h/2), \quad (5b)$$

The modified Borresen's scheme described in the above is incorporated into the 3-D neutron kinetics analysis code, CMSNACK, against which low-dimensional methods are tested.

2.2 The 1-D Two-Group Diffusion Equation

Considering that kinetics equations for thermal hydraulic feedback variables are also to be included in computation of the reactor transient problem, modelling of the transient neutronic behavior in three dimension is very costly in computer time. The 1-D method offers an improvement in computing cost. The equations to be solved in 1-D two-group model are

$$\frac{1}{v_1} \frac{\partial \phi_1(z,t)}{\partial t} = \frac{\partial}{\partial z} D_1 \frac{\partial \phi_1(z,t)}{\partial z} - \Sigma_{a1} \phi_1(z,t) + \frac{1-\beta}{k} (\upsilon \Sigma_{f1} \phi_1(z,t) + \upsilon \Sigma_{f2} \phi_2(z,t)) + \sum_d \lambda_d C_d(z,t), \quad (6a)$$

$$\frac{1}{v_2} \frac{\partial \phi_2(a,t)}{\partial t} = \frac{\partial}{\partial z} D_2 \frac{\partial \phi_2}{\partial z} - \Sigma_{a2} \phi_2(z,t) + \Sigma_r \phi_1(z,t), \quad (6b)$$

$$\frac{\partial C_d(z,t)}{\partial t} = \frac{\beta_d}{k} (\upsilon \Sigma_{f1} \phi_1(z,t) + \upsilon \Sigma_{f2} \phi_2(z,t)) - \lambda_d C_d(z,t) \quad (6c)$$

d=1, 2, 3,···, D

These equations can be obtained by integrating two group diffusion equations in three dimension over the radial plane perpendicular to the axial direction z. The integration process then leads to the 1-D two-group parameters related to the 3-D group flux, $\phi_g(x,y,z)$, by

$$\Sigma_{xg} = \frac{\int\int \Sigma_x(x,y,z) \phi_g(x,y,z) \, dxdy}{\int\int \phi_g(x,y,z) \, dxdy}, \quad (7a)$$

and

$$DB^2_g = \frac{\int\int\left(-D_g\frac{\partial^2\phi_g(x,y,z,t)}{\partial x^2} - D_g\frac{\partial^2\phi_g(x,y,z,t)}{\partial y^2}\right)dxdy}{\int\int\phi_g(x,y,z,t)dxdy} \quad (7b)$$

There are various approaches of solving Eq.(6) numerically. In this study a fine-mesh finite difference scheme is adopted to produce a 1-D two-group finite-difference diffusion theory kinetics code, ODTRAN, which is a acronym of One Dimensional Transient Neutronics code.

2.3 Point Kinetics Method

The point kinetics method offers the simplest kinetics model for reactor transient analysis. As in the case of the 1-D ODTRAN method, the method can be derived from two-group diffusion equation in three dimension by representing two group flux $\phi_g(r, t)$ as a product of a shape function $S_g(r, t)$ and an amplitude function N(t), i.e.,

$$\phi_g(r, t) = S_g(r, t)N(t) \quad (8)$$

Substitution of Eq.(8) into two-group diffusion equation and a series of mathematical manipulation lead to the point kinetics equation :

$$\frac{dN(t)}{dt} = A(t)N(t) + \sum_{i=1}^{D}\lambda_i C_i(t), \quad (9a)$$

$$\frac{dC_i(t)}{dt} = B_i(t)\,N(t) - \lambda_i C_i(t)\,; \quad (9b)$$

where

$$A(t) = \frac{\rho(t) - \beta(t)}{A(t)},\quad \beta(t) = \sum_{i=1}^{D}\beta_i(t),$$

$$B_i(t) = \frac{\beta_i(t)}{A(t)},\ i = 1,2,3,\cdots, D \quad (10)$$

where the point kinetics parameters are given by

$$\rho(t) = \frac{1}{G(t)}\int dV[-M + F_p + F_d]\,[S(r, t)], \quad (11a)$$

$$A(t) = \frac{1}{G(t)}\int dV[w(r, t)]^T[v]^{-1}[S(r,t)], \quad (11b)$$

$$\beta_i(t) = \frac{1}{G(t)}\int dV[w(r,t)^T[F_{di}]\,[S(r, t)], \quad (11c)$$

where

$$G(t) = \int dV[w(r, t)]^T[F_p + F_d]\,[S(r, t)], \quad (12a)$$

$$-[M(r, t)] = \begin{pmatrix} \nabla\cdot D_1\nabla - E_{al} & 0 \\ \Sigma_r & \nabla\cdot D_2\nabla - \Sigma_{a2}\end{pmatrix}, \quad (12b)$$

$$[F_p] = \upsilon(1-\beta)\begin{pmatrix}\upsilon\Sigma_{f1} & \upsilon\Sigma_{f2} \\ 0 & 0\end{pmatrix}, \quad (12c)$$

$$[F_d] = \begin{pmatrix}\beta\upsilon\Sigma_{f1} & \beta\upsilon\Sigma_{f2} \\ 0 & 0\end{pmatrix}, \quad (12d)$$

$$[v]^{-1} = \begin{pmatrix}1/v_1 & 1 \\ 0 & 1/v_2\end{pmatrix}, \quad (12e)$$

$[w(r,t)]^T = [w_1(r,t),\ w_2(r, t)]^T$; w_g = weighting functions

For numerical solution of the point kinetics equation, we adopted a third-order Hermite polynomial method(8). The polynomial solution method for point kinetics equation is then incorpoated into the kinetics code POTRAN, which stands for Point kinetics-based Transient Neutronics code.

3. Numerical Results and Discussions

For the purpose of comparing computational accuracy of the 1-D two-group diffusion theory method and the point kinetics method with the reference CMSNACK 3-D kinetics method, the ODTRAN and POTRAN codes are used for obtaining the low-dimensional transient solutions to the LRA-BWR kinetics benchmark problem.

The LRA-BWR problem corresponds to a simulated superprompt critical transient induced by sudden withdrawal of a control rod. Fig. 1 shows the horizontal and vertical sections of the LRA-BWR. The reactor core consists of four different fuel types. The transient is induced by complete ejection of a control rod in region "R" in 2 seconds. Table 1 lists a set of input data required for transient computations.

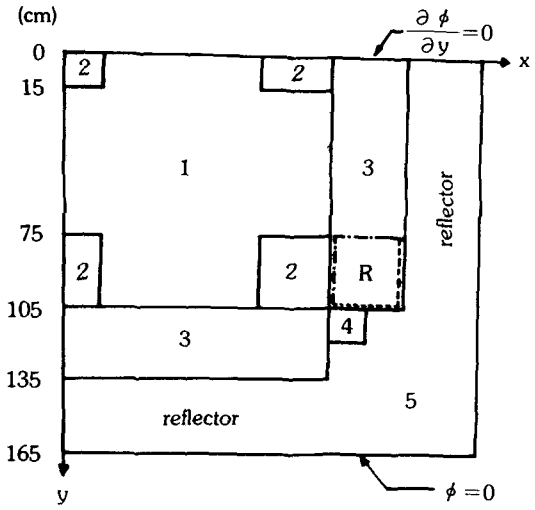

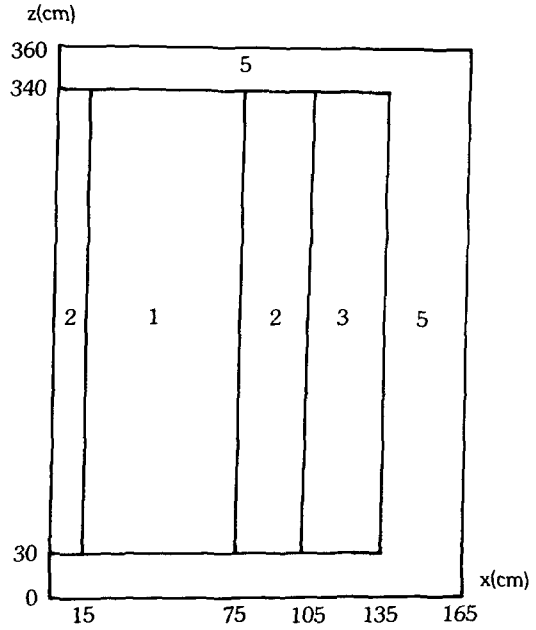

Fig.1. LRA-BWR (A) Horizontal Section (B) Vertical Section

It is straightforward procedure to perform the 3-D CMSNACK reference computation for the LRA-BWR problem using the data in Table 1. Yet it is necessary to reduce the input data to the form suitable for the ODTRAN and POTRAN computations in order to obtain the low-dimensional solutions. Presented in the following are procedures for the input prepation of the ODTRAN and POTRAN codes and the LRA-BWR solutions by these codes in comparison with the reference 3-D CMSNACK result.

3.1 The 1-D ODTRAN Computation

The fundamental unknowns of the ODTRAN

Table 1 (A) Two-Group Constants

Region	Material	Group, g	D (cm)	Σ_a (cm^{-1})	$\upsilon\Sigma_f$ (cm^{-1})	Σ_γ (cm^{-1})
1	Fuel 1 with Rod	1	1.255	0.008252	0.004602	0.02533
		2	0.211	0.1003	0.1092	
2	Fuel 1 *without* Rod	1	1.268	0.007181	0.004609	0.02767
		2	0.1902	0.07047	0.08675	
3	Fucl 2 with rod	1	1.259	0.008002	0.004663	0.02617
		2	0.2091	0.08344	0.1021	
4	Fuel 2 without rod	1	1.259	0.008002	0.004663	0.02617
		2	0.2091	0.073324	0.1021	
5	reflector	1	1.257	0.0006034	0.0	0.04754
		2	0.1592	0.01911	0.0	

Table 1(B)

Delayed Neutron Model		
group	β_i	$\lambda_i(sec^{-1})$
1	0.0054	0.0654
2	0.001087	1.35

Adiabatic Feedback Model

$$\frac{\partial T}{\partial t} = \alpha_1 \Sigma_f \phi$$

$$\Sigma_{a1}(t) = \Sigma_{a1}(0)[1 + \alpha_2(T(t)^{\frac{1}{2}} - 300^{\frac{1}{2}})]$$

$\alpha_1 = 3.83 \times 10^{-11}$ Kcm^3
$\alpha_2 = 3.3034 \times 10^{-3}$ K^{-2}

Energy Conversion

initial power density $= 10^{-6}$ W/cc
power $= \epsilon \int_{V_{core}} \Sigma_f \phi \, dV$
$\epsilon = 3.204 \times 10^{-11}$ W−sec/fission

code are the node–average group flux defined by

$$\phi_{gn}(t) = \frac{1}{h_n} \int_{z_{n-1}}^{z_n} \phi_g(z, t) \, dz.$$

The subscript n denotes the axial 1–D node with the width of h_n. Input data required for computing the $\phi_{gn}(t)$ are the two–group constants and the transverse buckling for each of 1–D nodes. In principle these can be computed using Eq.(7) in combination with a time–dependent 3–D flux. In practice, however, approximate schemes are inevitable since the time–dependent 3–D flux are *a priori* unknown.

One simple but straightforward method is to make use of steady state 3–D fluxes instead of the time–dependent flux. In this conjunction the steady state fluxes of interest are those for the core with all rods in, $\phi_g^{ARI}(x,y,z)$ and those for the core with all rods out, $\phi_g^{ARO}(x,y,z)$, which correspond to the initial and the final state of the LRA–BWR transient problem. Let's take the ϕ_g^{ARI} for instance. This flux can lead to the 1–D diffusion equation parameters by EQ.(7):

$$\Sigma_{xgn}^{ARI} = \frac{\int_{V_n} dxdy \, \Sigma_{xg}(x,y,z) \, \phi^{ARI}(x,y,z)}{\int dxdy \, \phi^{ARI}(x,y,z)} \qquad (14)$$

Needless to say, the $\phi_g^{ARO}(x,y,z)$ can result in the Σ^{ARO}. In the course of the LRA–BWR transient, the control rod may be located somewhere within the 1–D computational node n. Taking into account this situation, the node–dependent 1–D cross section may be approximated by

$$\Sigma_{xgn} = (1-f)\Sigma_{fgn}^{ARO} + f\Sigma_{fgn}^{ARI} \qquad (15a)$$

The "f" stands for the fraction of the control rod insertion into the node n. The transverse buckling may also be similarly approximated by

$$DB^2_{gun} = (1-f)\,(DB^2_{gun})^{ARO} + f(DB^2_{gun})^{ARI} \qquad (15b)$$

Table 2 shows the node–dependent two–group parameters derived from Eq.(14). The 3–D fluxes are obtained from the CMSNACK computions for the ARO and the ARI core with rectangular node of $15 \times 15 \times 30$ cm^3, which correspond to 10 axial nodes. It is noted that the two group parameters except for the top and the bottom nodes are almost the same irrespective of the nodes. This is due to the fact that either the ARO core or the ARI core has uniform material properties, which in turn suggests that 2–D fluxes can also be used for computing the Σ_{xyz}^{ARO} and Σ_{xyz}^{ARI}. Table 3 shows 1–D two group parameters derived from 2–D flux at ARI and ARO. It must be observed that there is little or no difference in numerical values of two group parameters of tables 2 and 3.

Two group parameters from Eq.(15) in combination with the data in Table 1 are put into the ODTRAN code for a 1–D solution to the LRA–BWR benchmark problem. Shown in Table 4 is comparison of a 3–D CMSNACK computation and 1–D ODTRAN solutions for the LRA–BWR problem. Fig. 2 also compares two computations in terms of transient core power density as funtion of time. As may be noted from these comparison, the 1–D ODTRAN computations predict the transient behaviour of the LRA–BWR in a fairly similar way as the 3–D CMSNACK computation, even though the former predict the timing of the first power peak a little bit earlier than the latter, and

Table 2(A) Homogenized 1D Cross Section with All Rods IN

n	D_g	Σ_{ag}	$\upsilon \Sigma_{fg}$	Σ_r	DB_g^2
1	.1259E+01	.9225E−02	.4629E−02		.1269E−02
	.2055E+00	.8527E−01	.1010E+00	.2610E−01	−.8038E−03
2	.1259E+01	.9225E−02	.4629E−02		.1269E−02
	.2055E+00	.8527E−01	.1010E+00	.2610E−01	−.8038E−03
3	.1259E+01	.9225E−02	.4629E−02		.1269E−02
	.2055E+00	.8527E−01	.1010E+00	.2610E−01	−.8038E−03
4	.1259E+01	.9225E−02	.4629E−02		.1269E−02
	.2055E+00	.8527E−01	.1010E+00	.2610E−01	−.8038E−03
5	.1259E+01	.9225E−02	.4629E−02		.1269E−02
	.2055E+00	.8527E−01	.1010E+00	.2610E−01	−.8038E−03
6	.1259E+01	.9225E−02	.4629E−02		.1269E−02
	.2055E+00	.8527E−01	.1010E+00	.2610E−01	−.8038E−03
7	.1259E+01	.9225E−02	.4629E−02		.1269E−02
	.2055E+00	.8527E−01	.1010E+00	.2610E−01	−.8038E−03
8	.1259E+01	.9225E−02	.4629E−02		.1269E−02
	.2055E+00	.8527E−01	.1010E+00	.2610E−01	−.8038E−03
9	.1259E+01	.9225E−02	.4629E−02		.1269E−02
	.2055E+00	.8527E−01	.1010E+00	.2610E−01	−.8038E−03
10	.1259E+01	.9225E−02	.4629E−02		.1269E−02
	.2055E+00	.8527E−01	.1010E+00	.2610E−01	−.8038E−03

Table 2(B) Homogenized 1D Cross Section All Rods OUT

n	D_g	Σ_{ag}	$\upsilon \Sigma_{fg}$	Σ_r	DB_g^2
1	.1259E+01	.9715E−02	.4635E−02		.1791E−02
	.2053E+00	.8133E−01	.1003E−00	.2620E−01	−.1079E−02
2	.1259E+01	.9715E−02	.4635E−02		.1791E−02
	.2053E+00	.8133E−01	.1003E−00	.2620E−01	−.1079E−02
3	.1259E+01	.9715E−02	.4635E−02		.1791E−02
	.2053E+00	.8133E−01	.1003E−00	.2620E−01	−.1079E−02
4	.1259E+01	.9715E−02	.4635E−02		.1791E−02
	.2053E+00	.8133E−01	.1003E−00	.2620E−01	−.1079E−02
5	.1259E+01	.9715E−02	.4635E−02		.1791E−02
	.2053E+00	.8133E−01	.1003E−00	.2620E−01	−.1079E−02
6	.1259E+01	.9715E−02	.4635E−02		.1791E−02
	.2053E+00	.8133E−01	.1003E−00	.2620E−01	−.1079E−02
7	.1259E+01	.9715E−02	.4635E−02		.1791E−02
	.2053E+00	.8133E−01	.1003E−00	.2620E−01	−.1079E−02
8	.1259E+01	.9715E−02	.4635E−02		.1791E−02
	.2053E+00	.8133E−01	.1003E−00	.2620E−01	−.1079E−02
9	.1259E+01	.9715E−02	.4635E−02		.1791E−02
	.2053E+00	.8133E−01	.1003E−00	.2620E−01	−.1079E−02
10	.1259E+01	.9715E−02	.4635E−02		.1791E−02
	.2053E+00	.8133E−01	.1003E−00	.2620E−01	−.1079E−02

Table 3(A). Homogenized 1D Cross Section with 2D Computation at ARI

n	D_g	Σ_{ag}	$\upsilon \Sigma_{fg}$	Σ_r	DB_g^2
1	.1259E+01	.9238E−02	.4629E−02		.1279E−02
	.2056E+00	.8533E−01	.1011E+00	.2609E−01	−.8196E−03

Table 3(B). Homogenized 1D Cross Section with 2D Calculation at ARO

n	D_g	Σ_{ag}	$\upsilon\,\Sigma_{fg}$	Σ_r	DB_g^2
1	.1259E+01	.9723E−02	.4635E−02		.1797E−02
	.2054E+00	.8144E−01	.1004E+00	.2619E−01	−.1096E−02

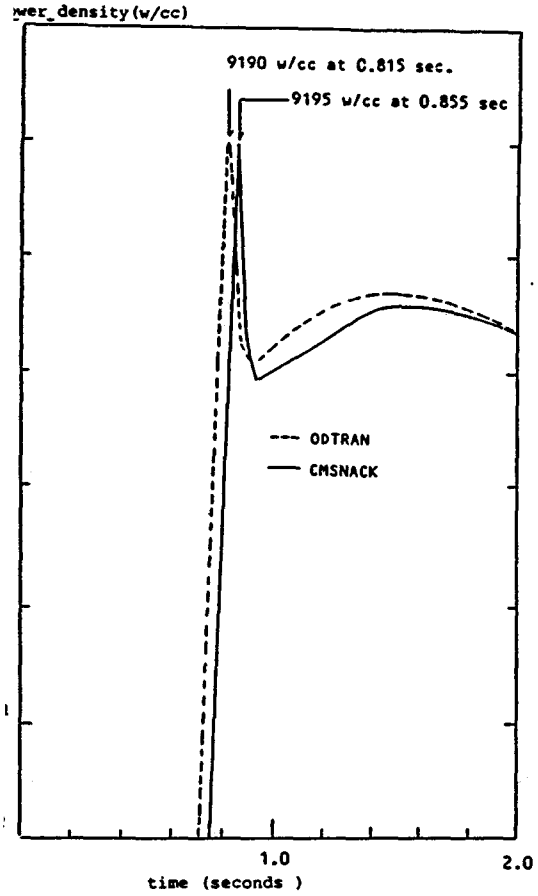

ig.2. Comparision of 1-D ODTRAN and 3-D CMSNACK Results for Transient Power Density

overestimate the power densities at 3 seconds after transient in comparison with the latter. It may also be noted that the reduction of the 1-D nodal width from 3 cm to 1 cm brings about little or no change in the computational results of the 1-D ODTRAN code. From the standpoint of computing time the 1-D ODTRAN code is extremely efficient. It should be observed that the 1-D ODTRAN code takes about 10 to 30 times less computing time than the 3-D CMSNACK code to solve the LRA-BWR problem.

3.2 The POTRAN Computation

The basic input parameters of the POTRAN code are the kinetics parameters $\rho(t)$, $\beta(t)$ and $\Lambda(t)$. Enumeration of these parameters by Eqs.(11) requires *a prior* knowledge on the weighting function $Wg(r, t)$ as well as the shape function $Sg(r,t)$. Since these functions are unknown *a priori*, approximate schemes are inevitable. The simplest of all approximations on the shape functions is so called the adiabatic approximation in which the shape function is assumed to be independent of time.

Taking $Wg(r,t)=1$ and $Sg(r, t)=Sg(r, t)=Sg(r, 0)$ under this approximation, the point kinetics parameters are computed by

$$\rho(t)=-\frac{1}{G(t)}\left[\sum_g \int \Sigma_{ag}(r, t)\,\phi_g(r, 0)dV - \sum_g \int \nabla\cdot D_g\nabla\phi_g(r, 0)dV\right], \quad (16a)$$

$$A(t)=\frac{1}{G(t)}\int \sum_g \frac{1}{v_g}\upsilon\,\Sigma_{fg}\phi_g(r, 9)dV, \quad (16b)$$

$$\beta_i(t)=\beta_i, \quad (16c)$$

$$G(t)=\int \sum_g \upsilon\,\Sigma_{fg}\phi_g(r, 0)dV. \quad (16d)$$

The $Sg(r, 0)$ is related to the time-independent flux $\phi_g(r, 0)$ by

$$\phi_g(r, 0)=S_g(r, 0)N(0)\ (N(0)=1).$$

Table 5 lists the numerical values of the point kinetics parameters by assuming $Sg(r, 0)=\phi_g(r, 0)$, which is the initial steady state flux of the LRA-BWR with all rods in. Eq.(16) defining the

Table 4. Comaparison of 1–D ODTRAN Computation with 3–D CMSNACK Results

Methods	CMSNACK	ODTRAN		
K for initial state	.997393	.997761	.997765	.997747
time to first peak(sec)	.855	.815	.815	.815
power at first peak(w/cc)	9195	9157	9190	9234
control rod position from bottom of core(cm)	127.5	122.3	122.3	122.3
time to second peak	1.443	1.461	1.454	1.419
power at second peak	458	501.4	501.2	500.1
control rod position from bottom of core(cm)	216.5	219.1	218.1	219
power at 3 seconds	74.2	91.5	91.8	92.2
CPU time(sec) MV–8000	5201	151	217	402

Table 5. Point Kinetics Parameters by Adiabatic Approximation

Parameter	Numerical values
$\rho(t)$	$1-\rho_1(t)-\rho_2(t)-\rho_2(t)$
A(t)	2.926×10^{-5} sec
$\beta_i(t)$	$\beta_1=0.0054$ $\beta_2=0.001087$

reactivity $\rho(t)$ can be rearranged in the following form :

$$\rho(t)=1-\left[\frac{1}{G(t)}\int_{S_R}\sum_g J_g dS + \frac{1}{G(t)}\int_{V_R}\Sigma_{a1}(t)\phi_1(r,0)dV + \frac{1}{G(t)}\int_{V_R}\Sigma_{a2}(t)\phi_2(r,0)dV\right]. \quad (17)$$

The $\rho_1(t)$, $\rho_2(t)$, and $\rho_3(t)$ in table 5 stand for three terms in the bracket in Eq.(17) in order. These three terms correspond to the loss of reactivity due to net leakage of neutrons, fast absorptions and thermal absorptions, respectively. Computation under the adiabatic approximation leads to

$$\rho_1(t)=,003355, \quad (18a)$$

$$\rho_2(t)=\rho_2(0)[1+\alpha(T^{\frac{1}{2}}-T_0^{\frac{1}{2}})],$$

$$\rho_2(0)=\frac{1}{G(t)}\int_{V_R}\Sigma_{a1}(0)\phi_1(r,0)dV = 0.2485, \quad (18b)$$

$$\rho_3(t)=\sum_{1=0}\rho_{31}\eta_1(t), \quad (18c)$$

where

$$\eta_1(t)=\begin{cases}\frac{t_{1+1}-t}{\Delta t} & t\in\left[\frac{1}{5}\ \frac{1+1}{5}\right],\\ \frac{t-t_1}{\Delta t} & t\in\left[\frac{1-1}{5}\ \frac{1}{5}\right],\\ 0 & t<\frac{1-1}{5},\ t>\frac{1+1}{5}.\end{cases}$$

It is noted that the 2 seconds of the rod withdrawal period is divided into 10 equal intervals in enumerating the $\rho(t)$. The coefficients of Eq.(18c) are given by Table 6.

As shown shortly, the adiabatic approximation fails to describe LRA–BWR transient adequately. The main reason for this failure is that the approximation can not follow the reactivity change induced by the rod withdrawal properly. To remedy this deficiency of the adiabatic approximation, therefore, a modified procedure is adopted. The procedure consists of computing the static reactivity as a function of control rod withdrawal position and representing the results by the amount of reactivity change equivalent to the control rod withdrawal. Fig.3 shows the 3–D CMSNACK computaion for the effective multiplication factor of LRA–BWR core as a function of control rod position. Since the rod is fully withdrawn in 2 seconds, the variation in k_{eff} is readily reduced to the corresponding reactivity change as a function

Table 6. Numerical values of Coefficients, φcx, ℓ

ℓ	0	1	2	3	4
ρ_{31}	0.7288	0.7283	0.7253	0.7190	0.7145
5	6	7	8	9	10
0.7119	0.7102	0.7090	0.7080	0.7072	0.7067

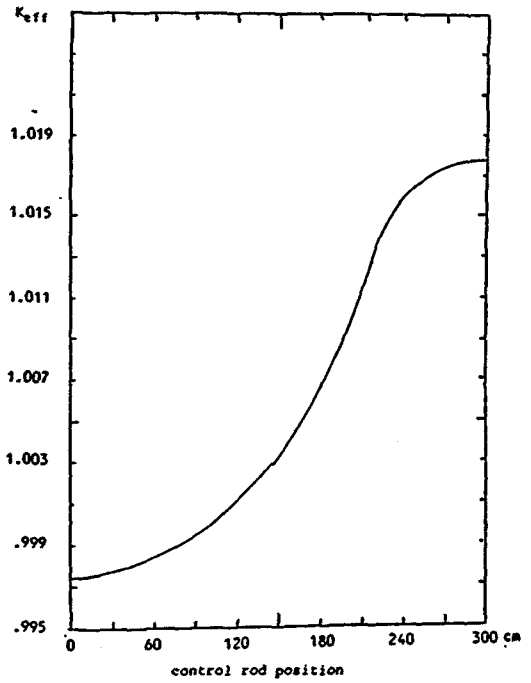

Fig.3. Variation of Keff. vs. Control Rod Position

of rod withdrawal time. In reducing the variation in the k_{eff} to the time-dependent reactivity change we observed that the sole effect of control rod movement is to change the thermal absorption cross section of the material region R in Fig. 1. With this observation we incorporated the reactivity change due to rod withdrawal int the $\rho_3(t)$ term in Eq.(17) by the following equation

$$\rho_3(t) = \rho_3(0) + \rho_{cx}(t). \quad (19)$$

The $\rho_{cx}(t)$ is then determined so that the variation of the k_{eff} in Fig.3 is simulated by Eq.(18) in combination with Eq.(17). The results are given in the form of piecewise interpolation :

$$\rho_{cx}(t) = \sum_{l=0}^{10} \Delta\rho_{cxl}\,\eta_l(t).$$

The coefficients are given in Table 7.

Table 7. Numerical values of Coefficients, ρcx, ℓ

ℓ	0	1	2	3	4
ρ_{cxl}	0.	0.4755	15.439	47.195	46.864
5	6	7	8	9	10
32.697	22.108	15.118	10.389	6.2778	1.9342

The point kinetics parameters obtained in the above are used to obtain the point kintcis solution to the LRA-BWR kinetics problem by the POT-

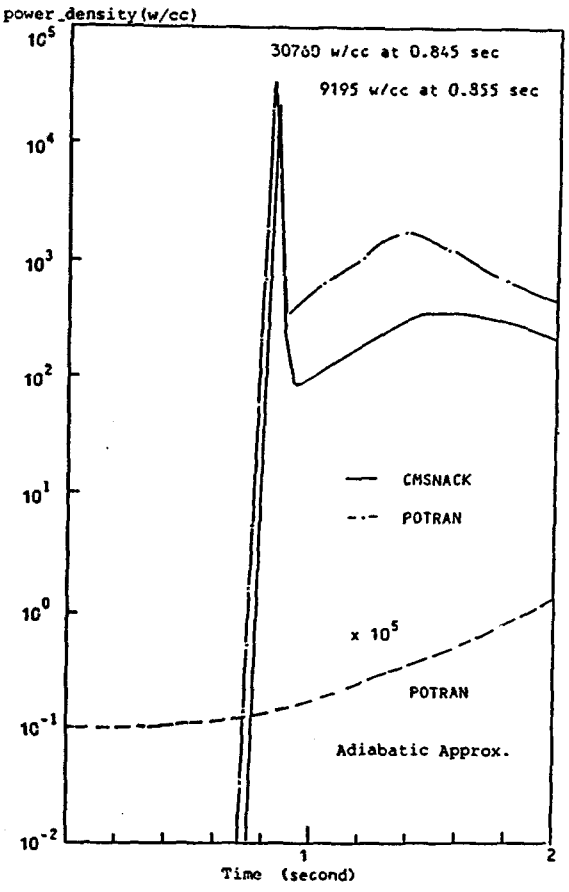

Fig.4. Comparison of POTRAN and 3-D CMSNACK results for Transient Power Density

Table 8. Comaparison of POTRAN Computation with 3–D CMSNACK Results

Transient Parameters / Methods	CMSNACK	POTRAN
K for initial state	.997393	
time to first peak(sec)	.855	,845
power at first peak(w/cc)	9195	30760
control rod position from bottom of core(cm)	127.5	126.8
time to second peak	1.443	1.293
power at second peak	458	1084
control rod position from bottom of core(cm)	216.5	194
power at 3 seconds	74.2	1350
CPU time (sec) MV–8000	5201	77

RAN code. Table 8 and Fig.4 compare the POTRAN results with the 3–D CMSNACK computation. As mentioned already, the point kinetics parameters obtained by adiabatic approximation get nowhere in describing LRA–BWR transients. On the other hand, the modification of the reactivity parameter in accordance with static reactivity change with rod withdrawal gives rise to the POTRAN solution which is closer to the 3–D reference CMSNACK computation. It is seen that the POTRAN computation describes the overall transient behaviour of LRA–BWR in a similar way as the reference 3–D computation, yet discrepancies are observed in predictions of the core peak power and the fuel temperature. This is regarded as the limitation of the point kinetics model in so far as the kinetics parameters are derived by the approximate schems as adopted in this study.

4. Conclusion

The comparison of the low dimensional kinetics methods with the refernce 3–D method shows both limitation and advantage of the former methods. Needless to say, the main advantage of low–dimensioal kinetics methods lies in the fast computing speed. As shown clearly in Tables 4 and 8, the 1–D ODTRAN and the POTRAN codes are faster one or two order than the 3–D CMSNACK code. This is why the low dimensional methods are adopted in the safety analysis of the power reactors. In spite of this advantage, limitation of these low–dimensional method should not be overlooked. Among other things, the low–dimensional method requires careful procedure of input preparation in order to ensure reasonably acceptable accuracy.

In the applications of 1–D ODTRAN method to the rod ejection transients like the LRA–BWR problem the flux volume weighting scheme with a combined usage of static 3–D fluxes in ARI and ARO core configurations turns out to be satisfactory. This suggests the possibility of deriving another 1–D kinetics method using time–dependent synthesis method, which to be pursued in future study. In the case of the point kinetics POTRAN code, the adiabatic approximation may be useful in enumerating such parameters as β and Λ. Yet the reactivity parameter should be derived so that the reactivity change in the course of rod withdrawal is adequately simulated. The experience in this study suggests that computations of the static reactivity change provides a simple but practical way to get the reactivity parameter to be used in the POTRAN applications.

References

1. D. H. RISHER, JR, "An Evaluation of the Rod Ejection Accident in Westinghouse Pressurized Water Reactor Using Spatial Kinetics Methods," WCAP-7588(1971).
2. H.S. Cheng et. al., "The Use of MEKIN-B for LWR Transient Calculations," BNL-NUREG-28785(Nov. 1980).
3. Chen-Kwo Tsai, "Three Dimensional Effects in Analysis of PWR Steam Line Break Accident," Ph. D. Thesis, MIT(1985).
4. L.J. Agee, "RETRAN-02 A Program For Transient Thermal-Hydraulic Analysis of Complex Fluid Flow System," EPRI NP-1850(1981).
5. V.H. Ransom, et. al., "RELAP 5/MOD1.5; Models, development Assessment, and User Information," *INEL EGG-MSMD-6035(1982).*
6. J.M. Holzer, R. Habert and E.E. Pilat, "Consistency Considerations in the Use of Point Kinetics For BWR Application," Proc. of the First International RETRAN Meeting(Sep. 1980).
7. Argonne Code Center, Benchmark Problem Book, ANL-7416, Supplement 2(1977).
8. Kueng Yeh, "Polynomial Approach to Reactor Kinetics Equations," Nucl. Sci. Eng. Vol. 66, p.235(1978).
9. Chang Hyo Kim and Jong Hwa Chang, "A modified Borresen's Coarse-Mesh Method for a Spatial Neutron Kinetics Problem of Light Water Reactor," Proc. of the Topical Meeting on Reactor Physics and Safety, Saratoga Springs, NY Vol.1 p.563(1986).
10. D.E. Billington, et. al., "Survey of Results of a One-Dimensional Kinetic Benchmark Problem Typical for a Thermal Reactor," Proc. of the Joint NEACRP/CSNI Specialists' Meeting on New Developments in Three-Dimensional *Kinetics and Review of Kinetics Benchmark* Calculations, Garching, West Germany, 323(1975).